Encapsulating Tin Dioxide Nanoparticles into COF to Develop High Capacity Lithium Ion Battery Anodes

A thesis submitted towards the partial fulfilment of Integrated PhD degree program

By
Liya S Leo
20192020

Under the guidance of
Dr Ramanathan Vaidhyanathan
Professor

Department of Chemistry
Indian Institute of Science Education and Research
Dr Homi Bhabha Road, Pashan, Pune

Certificate

This is to certify that this dissertation "*Encapsulating Tin Dioxide Nanoparticles into COF to Develop High Capacity Lithium Ion Battery Anodes"* towards the partial fulfilment of the Integrated PhD programme at the Indian Institute of Science Education and Research, Pune represents work carried out by Liya S Leo at Indian Institute of Science Education and Research under the supervision of Dr. Ramanathan Vaidhyanathan, Professor, Department of Chemistry, during the academic year 2021-2022.

Signature of student

Date: 31-01-2023

Signature of Supervisor

Date

Declaration

I hereby declare that the matter embodied in the report entitled "*Encapsulating Tin Dioxide Nanoparticles into COF to Develop High Capacity Lithium Ion Battery Anodes"* are the results of the work carried out by me at the Department of Chemistry, Indian Institute of Science Education and Research, Pune, under the supervision of Dr Ramanathan Vaidhyanathan and the same has not been submitted elsewhere for any other degree.

Signature of student

Date: 31-01-2023

Signature of Supervisor

Date: 31-01-2023

Acknowledgement

I am thankful to everyone who has been with me throughout this journey. I would not have been able to submit this thesis without their help, guidance and support.

First and foremost, I would like to express my sincere gratitude to Dr. R. Vaidhyanathan, who is more than just my thesis supervisor. I sincerely thank him for believing in me, caring for me and for providing me the opportunity to work under his guidance and for supporting me throughout the project.

I would like to thank the honorable director of IISER Pune and all the staffs here for facilitating the smooth conduct of research work. Thanks to all my lab mates, Rinku, Deepak, Himan, Chandana, Pragalbh, Chitvan, Piyush, Rahul and Aleena for their support throughout this journey. Finally, I thank my family members and friends for being with me at all times. I am blessed to have a terrific friend circle at IISER Pune, who were a constant source of fun, care and motivation. Thanks for making my IISER life colorful. And I thank Almighty; this project would not have been completed without the help of the Almighty himself.

Table of Contents

Abstract

Covalent Organic Frameworks (COFs) are porous crystalline polymers formed by organic linkers connected through covalent bonds. They have numerous advantages such as high porosity, controllable pore size, thermal stability, functional tunability and low solubility in electrolyte. COFs have attracted wide attention due to their robust network, enhanced stability and open pores that will aid the inclusion of electrolyte ions when used as electrodes in LIBs. In recent years, COFs have attracted a lot of attention as prospective anode materials for rechargeable batteries due to their structural diversity and atomic-level functional adaptability. We have already demonstrated that COF have the potential to deliver excellent rate-performance for LIBs, but their ion-storage capacity needs to be further improved to achieve practical energy densities.

Incorporating metal nanoparticles into the COFs and employing this as an electrode will help to enhance ionic or electrical conductivity for LIBs. Owing to their high theoretical specific capacity, tin dioxide is considered as a potential LIB anode. However, due to the severe agglomeration and significant volume fluctuations of SnO_2 particles during the Li intercalation de-intercalation, its use in real lithium-ion batteries is still constrained. Aggregation of particles result in poor electrochemical performance as it restricts the availability of active sites for Li^+ ions and huge volume changes lead to electrode cracking which in turn restricts the cycling capability of electrodes. An effective approach to solve the above problems is either reduces the size of SnO_2 particles and provides a support that can disperse these particles and mitigate the associated volume changes. The nano confinement of the SnO_2 particles in the COF would prevent their coagulative growth into undesirable sizes, which can lead to electrode cracking. Here we have used COF namely, IISERP-COF6 as the porous support which was successful in dispersing tin dioxide as SnO_2 nanoparticles. This SnO_2 loaded IISERP-COF6 was employed as the anode material for LIB and this composite exhibited a specific capacity of 1100 mAh/g at 100 mA/g current density.

Chapter 1: Introduction

A potential family of organic porous materials with highly ordered and periodic network architectures is covalent-organic frameworks (COFs). COFs have the advantage of being structurally predesignable, synthesizable, and functionally manageable, which distinguishes them from other polymers. Crystallinity is a key feature of these organic porous materials.[1] COFs basically integrate organic building blocks into a periodically ordered and extended 2D/3D polymers to generate highly ordered well defined lattices. The designing of COF enables one to predesign primary- and high-order structures, considerably boosting our capacity to design organic compounds to yield structures that are predictable with specific features and desirable functionalities. Due to their highly ordered porous structures, large specific surface area, excellent chemical stability and adjustable functionalities, COFs are potential candidates for different applications such as energy storage and conversion (water splitting, batteries, supercapacitors etc.), gas storage and separation, adsorption, catalysis etc.[2]

1.1 Basic principle behind formation of COFs

The structure of the COFs is solely determined by the monomers used. Hence, we can predesign and synthetically control the structure of COF. COFs employ step-growth polymerization for chain propagation between the chosen organic monomers 2D or 3D manner.[3] This ensures that the rigid framework are topologically directed to assure well defined ordered structures. Covalent interactions and noncovalent interactions are involved throughout polymerization process to create well-defined, crystalline structures.[1]

Other than self-condensation, the creation of COFs needs minimum two monomers, one will acts as a knot and the other as a linker. The knots are positioned at the branch sites, where they form polygonal backbones by joining with the linkers via covalent bonds. Other than reactive sites, desirable functionalities could be incorporated into the monomers for pore wall interface engineering. Thus, the organic monomers not only determine the framework structure, it also enables us to construct COF with desirable functionalities.[4] In designing COFs, Various geometries of knots and linkers are merged to produce extended polygonal structures. The topology diagram for the design of 2D and 3D COFs are given in Fig.1.(A,B).

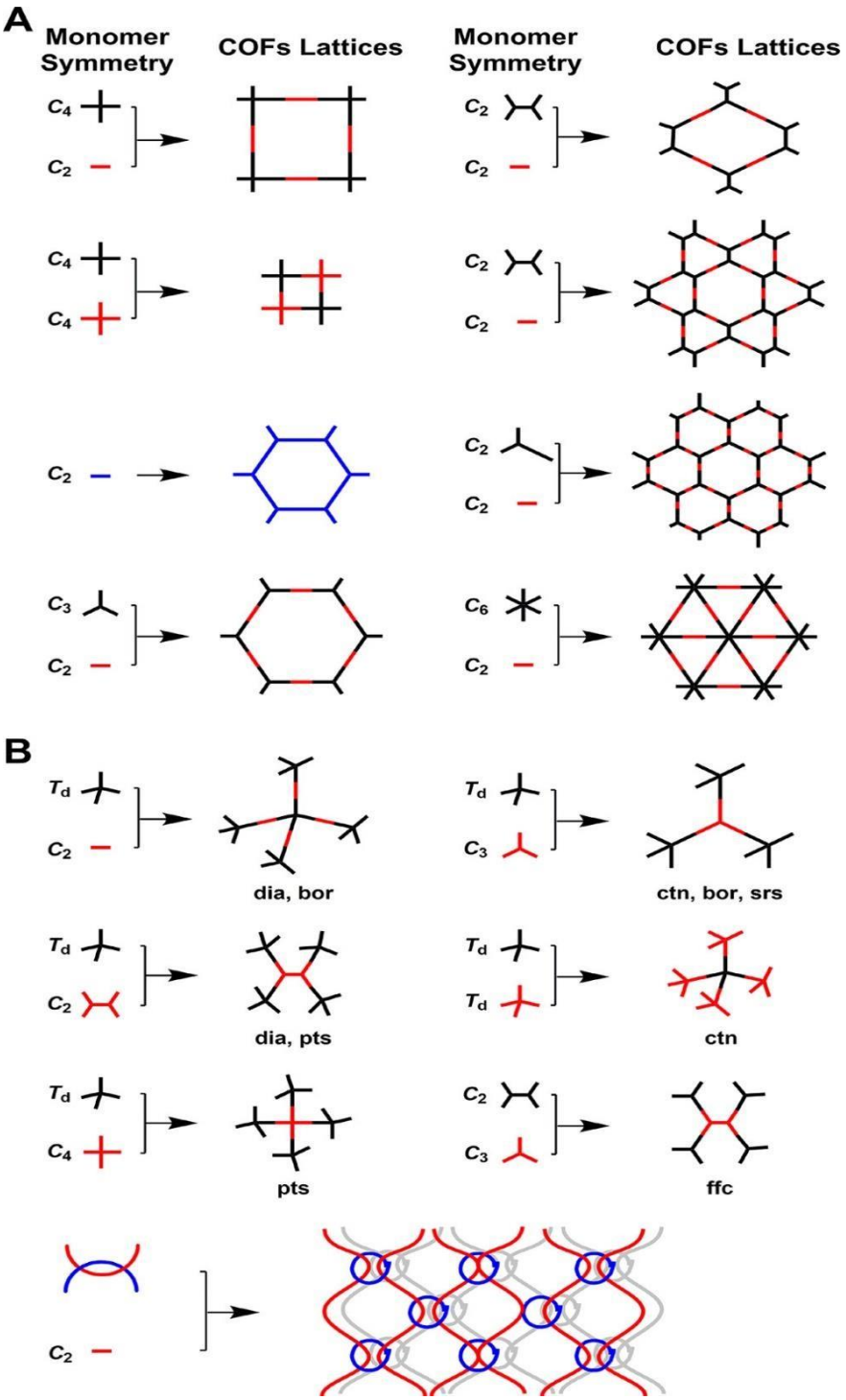

Fig 1 (A, B) Topology diagram for 2D and 3D COFs design[1].

Tuning of pore size, pore aperture and pore wall interfaces is crucial in designing COFs for various applications. The substantial structural diversity that may be gained by carefully choosing the organic monomers utilized to create COFs is one of its appealing qualities.[5] Intrinsic porosity, precise pore aperture, ordered channels, substantial surface area, high pore volume, low density, excellent

chemical and thermal stability and designable functionality makes COFs attractive materials for application such as catalysis, optoelectronics, gas adsorption, and electrochemical applications such as battery, supercapacitors, electrocatalysis etc.[3]

1.2 COFs for electrochemical applications

In the light of the demand for renewable and clean energy, numerous studies have switched their focus to the use of porous materials for electrochemical energy storage and conversion. Thus the development of COF-based materials for electrochemical applications, such as electrocatalysts for HER, OER, ORR, electrode materials for primary and secondary batteries (LIBS, NABs, ZABs) have gained a lot of attention in this regard.[6]

COFs have shown some appealing characteristics, which make it an amazing candidate for electrochemical applications. One important feature is it has great structural control. The functionalities can be tuned according to the electrochemical application by selection of appropriate organic monomers. Since they are completely composed of organic monomers joined by covalent bonds, several COFs will have π-conjugated frameworks and hence exhibit decent crystallinity. Also, the enormous surface areas and pore volume in COF ensures a high number of accessible catalytic sites. Good chemical and electrochemical stability assure decent durability for electrochemical devices.[7]

Incorporating metal ions into COFs will help in dispersing these metal ions into pores as nanoparticles and thus increases the efficiency of the material as electrodes in batteries and supercapacitors. Introduction of redox active sites in COFs will increase their efficiency as electrodes in batteries and supercapacitors. Introducing functional groups or metal sites into COFs will improve their electrochemical performance (Fig 2). Regular pore channels in COF will aid unhindered mass transfer which is crucial for electrocatalytic applications. High conjugation in COFs will enhance electronic conductivity in electrochemical energy storage process. Redox active sites in COFs will enhance the kinetics which helps in increasing the capacity.[8]

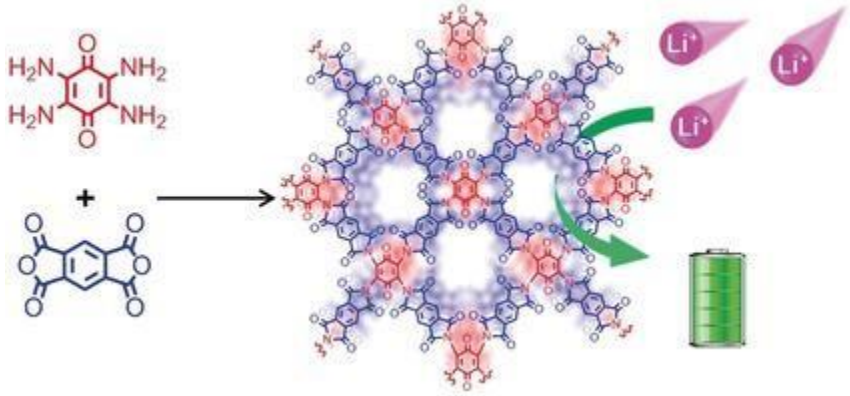

Fig.2 COF with redox active groups that can interact with Li ions in LIB.[29]

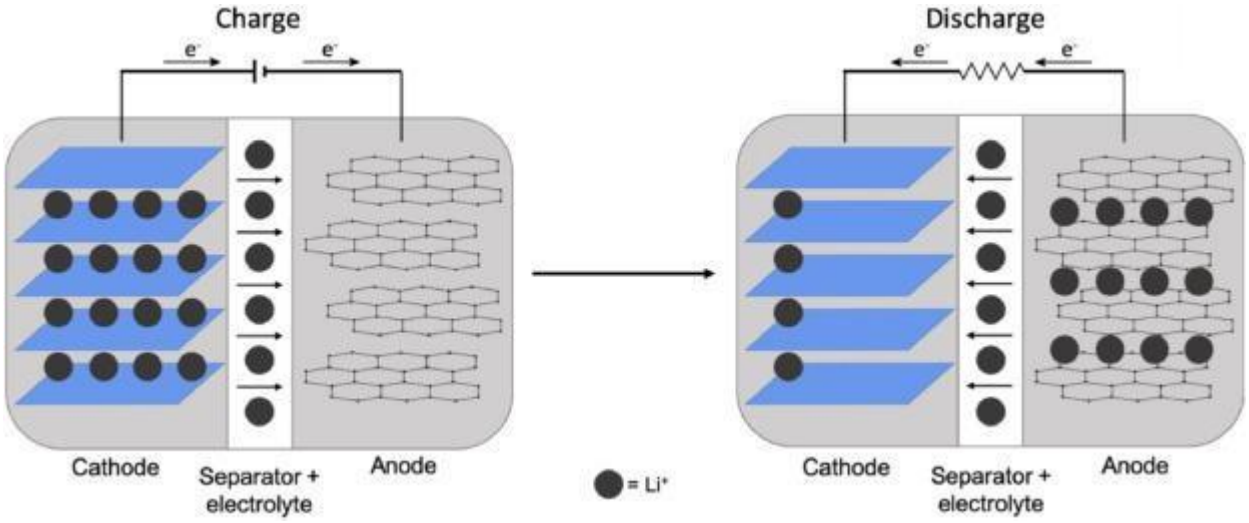

Fig.3. Diagram depicting movement of ions during charge discharge[30]

1.2.1 Covalent Organic Frameworks for LIBs

One among the most popular energy storages in the current world are LIBs, broadly employed in various compact electronic devices. With their high energy density, high voltage, compactness and durability, LIBs dominate the portable electronics sector. But the current produced LIBs have to be significantly improved in terms of their capacity to meet the growing demands for renewable energy. Cost, Safety and boosting the capacity and energy density are some of the areas where we should focus more to improve LIB performances.[9]

There are three important components in a LIB, namely cathode, anode and separator (usually a polymer membrane that will be soaked in the electrolyte). Tuning the material properties of all these components will have a profound impact in the overall battery performance. During charging, Li ions are released by the cathode and they move across the electrolyte and intercalate into the anode layers, generating flow of electrons from cathode to anode, which moves through the external circuit. Fig.3 shows the movement of ions during charge/discharge in a LIB with COF as the anode material. During discharging, the opposite happens. Since the ions are stored in the electrode, to build high power density battery, it is essential to have electrodes with high specific capacity. Commonly used anode in LIBs is graphite and a lithium transition metal oxide such as $LiCoO_2$ or $LiMn_2O_4$ is generally used as the cathode. Though graphite is commonly employed as the anode material in LIB, their theoretical specific capacity is just 372 mAh/g which is not sufficient to meet the growing energy demands. So, we have to think about alternative materials for anodes in LIBs.[10]

COFs are promising materials in this regard as they have layered conjugated structures like graphene. Also, unlike graphene, their properties can be tuned at the molecular level. COFs, with their intact framework, chemical tunabilty, high porosity, large internal surface area, abundant customizable pores, low densities, excellent stability are favorable materials for LIB anodes. When COFs are used as anodes, it should be able to provide high output voltage, high capacity and cycling stability which

can contribute to high energy density of LIBs. Incorporating redox active moieties into judiciously designed COFs is an effective approach to increase the capacity. Introducing multiple redox active groups (like CN and CO groups) into COF, doping the COF framework with N, O atoms are some of the strategies that can be adopted to enhance the battery performance of these materials[3](Fig.4A). Exfoliation of COF is another strategy to improve the performance of LIB (Fig. 4B,C). A metal modification technique that incorporates metal active sites into COFs by strong coordination interactions of organic building blocks with metal species is another effective method for COF functionalization. Some of the things that should be considered while incorporating metal ions into covalent organic frameworks are whether the binding energies between metals and COFs are strong enough to allow for stable combination, whether the incorporation of metal species will alter the structural properties of COFs.

Due to their high theoretical capacities, elements such as Germanium (Ge), Tin (Sn), Silicon (Si) are also potential candidates for improving the LIB performance when employed as anode. Some of their intrinsic features like very high volumetric and gravimetric capacity, natural abundance remains as the highlight features that make this a good candidate for LIBs.[11] However, the huge change in volume that occur during the Li^+ intercalation and de intercalation, can end up in a significant irreversible capacity loss and short cycle life, severely limiting their practical uses. Compared to tin, Ge and Si suffers from a greater volume expansion which in turn will result in electrode pulverization resulting in capacity fading and low coulombic efficiency. Thus, among Si, Ge and Sn, Sn seems to be a better material as it suffers from low volume change compared to Si and Ge.[11]

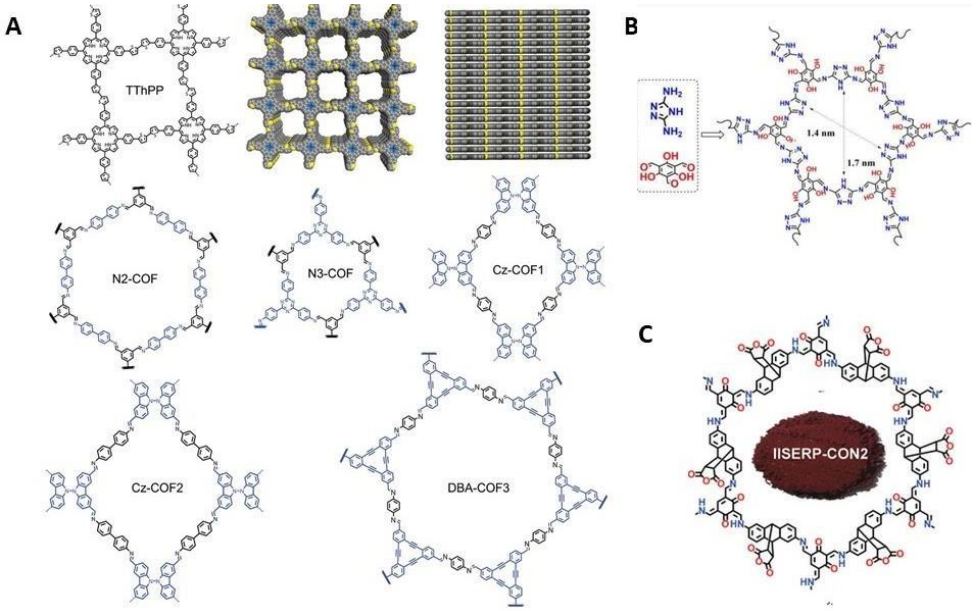

Fig.4. A. Various COF linkages and chemistries used for anode in LIB[30]. (B) IISERP-CON1, an imine based CON employed as anode in LIB[33]. (C) A chemically exfoliated COF showing high specific capacity anodic character with rapid diffusion of Li ions enabling high rate performance[34].

1.3 Tin based anodes for LIBs

When we are using tin as the anode material, one has to think about effective solutions that can mitigate the volume change. A few effective approaches are (1) lowering mechanical strain by reducing particle size to the nanoscale (2) confining the metal on to a porous framework so as to create a stable SEI layer and the interior pore must have enough room for Sn to expand. (3) nanosized Sn can be dispersed in a conductive matrix.[12]

1.3.1 Tin Dioxide based materials as anodes for LIBs

SnO_2 based anode is a better alternative to graphite in lithium-ion batteries as the theoretical specific capacity of SnO_2 is way higher than graphite. Coming into the electrochemistry, when used as anode material in LIB, First, in the conversion reaction, SnO_2 will react with Li^+ to form Li_2O and Sn. The theoretical capacity of this reaction alone is 711mAh/g. However, this process is thought to be irreversible, therefore not contributing to the battery capacity.[13] This is the primary cause of the substantial capacity degradation of SnO_2 during the initial lithiation phase. The following is the chemical reaction:

$SnO_2 + 4Li^+ + 4e^- \rightarrow Sn + 2Li_2O$

After the conversion reaction, alloying reaction takes place. During alloying reaction, the Sn formed in the above reaction alloys with Li^+ to form Li_xSn alloy. This process with a theoretical capacity of 783 mAh/g is reversible and yields to the specific capacity of the anode material in battery. This process depicts the charging discharging process of anode in LIB.

$Sn + xLi^+ + xe^- \leftrightarrow LixSn\ (0 \leq x \leq 4.4)$

But huge volume changes, pulverization and continuous SEI layer formation takes place during this alloying dealloying process leading to severe capacity loss and limited cycle life. Therefore, it is important to come up with structures that can mitigate this volume changes associated with alloying/dealloying process, which can help in improving the overall specific capacity of the battery. When the SnO_2 anode material is reduced to nanosized materials, it will have the advantage of shortened diffusion distance (for Li^+ and e^-) and reduce the magnitude of volume changes during the process.[13]Also, it has been reported that when SnO_2 is reduced to nanoparticles, there is a chance that the conversion reaction can become partially or completely reversible which thereby enhances the total specific capacity of the material.[14]Also supporting the SnO_2 nanoparticles into porous support will add to the advantage of buffering the volume changes associated with the alloying/ dealloying process.

In this work, we are aiming at taking the advantage of nanosized SnO_2 particles in a porous support namely, Covalent Organic framework (COF). The pores in the COF allows homogenous distribution of tin dioxide nanoparticles and will also help in buffering the volume changes associated with alloying/dealloying process. Fig.5 depicts the advantage of using a porous support for tin dioxide when used as anode in a LIB.

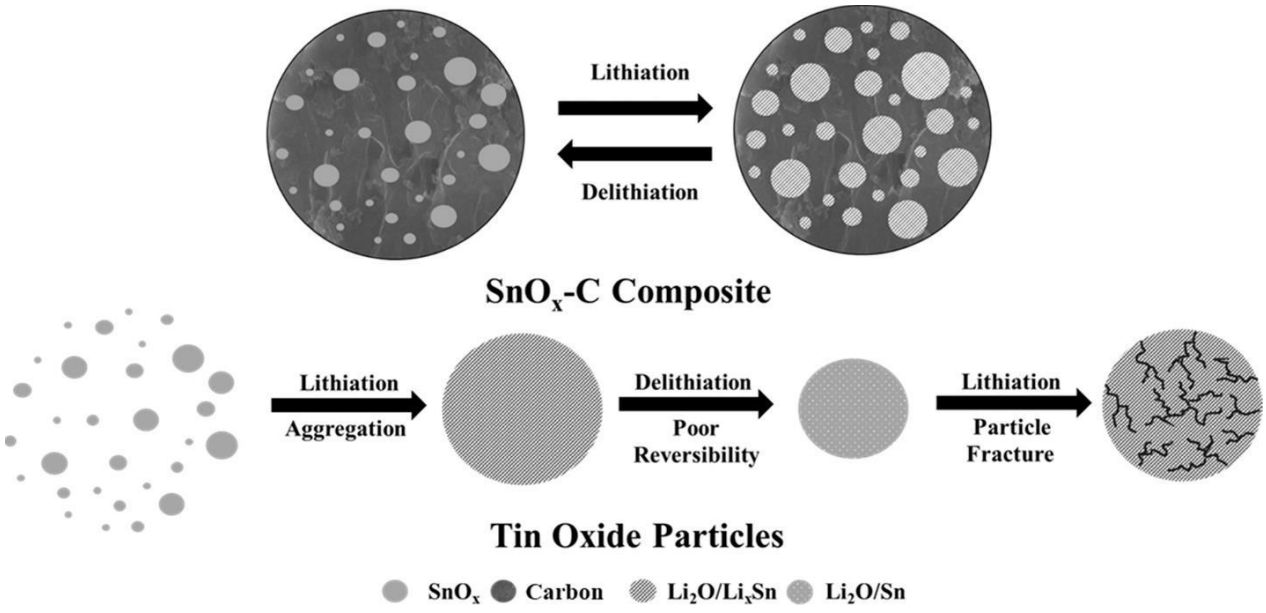

Fig.5. Scheme showing the lithiation- delithiation process of SnOx -C composite vs tin dioxide particles.[32]

Chapter 2: Methods and Instrumentation

2.1 Chemicals

All the chemicals like Tin(II) chloride, 4-hydroxy Benzaldehyde, Cyanuric chloride, Sodium hydroxide have been used without purification on purchase from Sigma Aldrich. Distilled water, Hexane, Methanol, Mesitylene and Dioxane are the solvents used.

2.2 Solvothermal Synthesis

High-quality COFs have frequently been built using the solvothermal method. This method depends on choosing the right solvent for the reaction media. In particular, the kind of solvent, the precursors' solubility, temperature, and time are thought to be significant variables that influence the crystallinity and porosity of COFs formed. Here we have synthesized COFs in autoclaves which can provide autogenous pressure and allow slow crystallization of COF with proper porosity. The monomers will be mixed with a particular solvent combination and will be heated over a duration of 3-7 days at a temperature of 80-120° C in a sealed pyrex tube or autoclave.

2.3 Analytical Characterization

Powder X-ray Diffraction

Powder X-Ray Diffraction data were recorded out using Rigaku Miniflex-600 instrument with Cu Kα (λ = 1.541 Å) and processed using PDXL software.

Adsorption

Gas adsorption was performed using a 3-FLEX pore and surface area analyzer and few cases using Micromeritics ASAP. Prior to adsorption, the samples were soaked in methanol for solvent exchange and evacuation**.** Samples were activated under 10^{-4}-10^{-5} Torr vacuum at 150°C for 12 hrs to 24hrs.

Field Emission Scanning Electron Microscopy

FE-SEM images were collected using Ultra Plus Field Emission Scanning Electron Microscope with integral charge compensator and embedded EsB and AsB detectors. Oxford X-max instruments 80 mm^2. (Carl Zeiss NTS, Gmbh), Imaging conditions: 2 kV, WD=2 mm, 200 kX, Inlens detector. For SEM analysis, the samples were dispersed in THF and were sonicated for 1hour. After that the well dispersed sample in THF were drop casted on silica wafer and dried in vacuum.

Infra Red Spectroscopy (IR spectroscopy)

IR spectra were recorded using a Nicolet ID5 attenuated total reflectance IR spectrometer in a range of 4000-600 cm^{-1} which operates at ambient temperature.

Nuclear Magnetic Resonance Spectroscopy (NMR)

NMR spectra for the products were recorded on 400 MHz Jeol ECS-400, Bruker 400 MHz instruments.

Electrochemical Measurements

Glove Box

The coin cell was fabricated under inert atmosphere inside MBRAUN UNIlab pro glovebox.

Cyclic Voltammetry (CV) and Galvanostatic charge discharge

The AMETEK Battery Analyzer was used to perform the constant current charge-discharge and CV measurements with VERSA STUDIO (Version 2.52) software.

Chapter 3: Synthesis and Characterization of Anode material

Synthesis and Characterization of SnO_2 @IISERP-COF6

3.1 Synthesis

3.1.1 Synthesis of 2,4,6-Tris (4-formyl phenoxy)-1,3,5- triazine

To a 100ml round bottom flask, at 0°C, 1.24g of NaOH (30.6mmol), 4-hydroxybenzaldehyde (3.72g) were added. To this reaction mixture, 30 ml of acetone and 30 ml of water was added as the solvent. To this reaction mixture, 1.84g of Cyanuric chloride dissolved in 30 ml acetone solution was added slowly. The reaction was kept under stirring in ice bath for 3 hrs. After 3 hrs, 200 ml of deionized water was added to the reaction mixture. An off-white-colored precipitate was formed upon adding. (Scheme 1). The product (Fig.1) obtained was thoroughly washed and dried. [15]

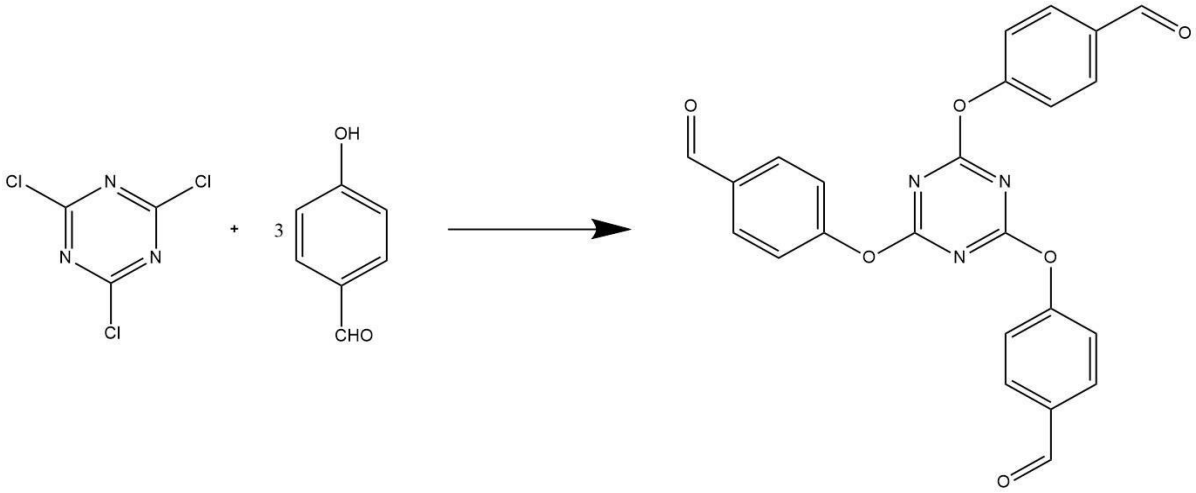

Scheme 1: Schematic diagram of synthesis of 2,4,6-Tris (4-formyl phenoxy)1,3,5- triazine

3.1.2 Synthesis of IISERP-COF6

IISERP-COF6 was synthesized using the solvothermal method in an autoclave. 198.7mg (0.45mmol)

of 2,4,6-tris (4-formyl phenoxy)1,3,5- triazine and 42 µL (0.68 mmol) of hydrazine hydrate (80 %) were dissolved in 3 ml mesitylene and 3 ml dioxane solvent mixture. The reaction mixture was stirred for half an hour. After 30 mins, 200 µL of glacial acetic acid was added to the reaction mixture and stirred again for 30 mins. Then the mixture was frozen in liquid nitrogen and kept in the oven for 3 days at 120°C. (Scheme 2). The product formed was collected by vacuum filtration, washed with methanol and dried.

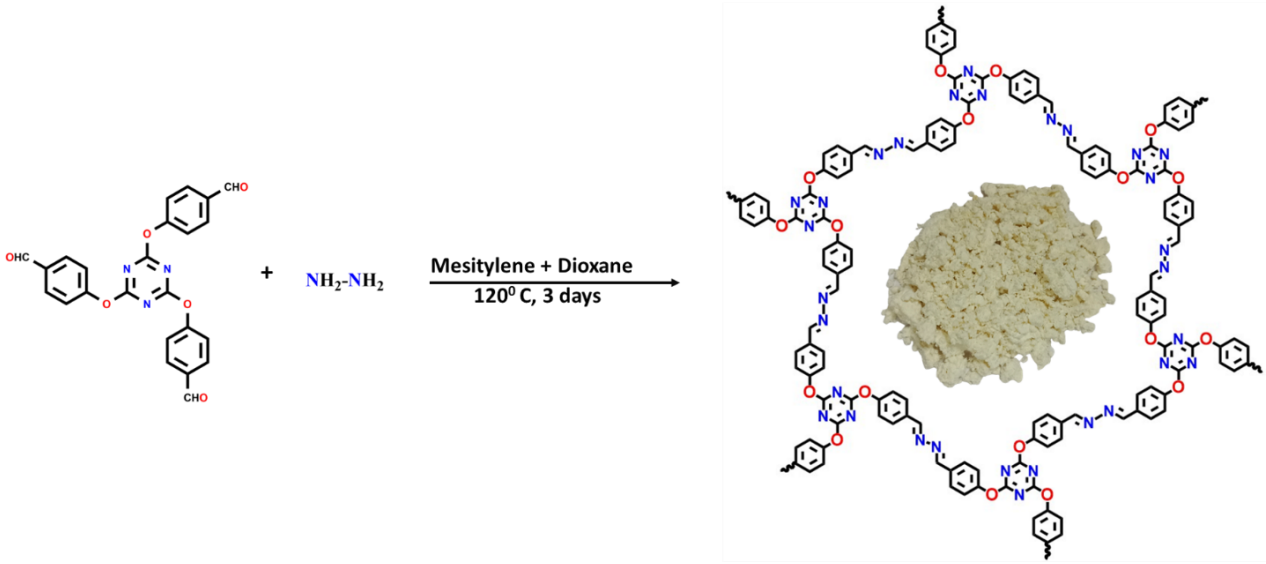

Scheme 2. Schematic diagram of synthesis of IISERP-COF6

3.1.3 Synthesis of SnO_2 loaded in IISERP-COF6 using double solvent method

Double solvent method has been used to load SnO_2 in IISERP-COF6.[17] 100 mg of IISERP-COF6 was dispersed in 40 ml hexane. The mixture was then sonicated for 30 mins. To this solution, a clear methanolic solution of $SnCl_2$ (42mg in 0.2ml) was added very slowly for 3 hrs with proper stirring. It was the kept under stirring overnight at room temperature. After 12hrs, the solvent was decanted. The solid was then heated at 150°C for 12 hr. The dried solid was then suspended in 20 ml of water (after cooling down to room temperature) and then it was reduced by adding 30 ml of freshly prepared 0.1M aq. $NaBH_4$ solution (111 mg) under vigorous stirring and then washed thoroughly with water. Scheme 3 Shows the process of SnO_2 loading. The synthesized SnO_2@IISERPCOF was then characterized and then used as active material for anode material for LIB.

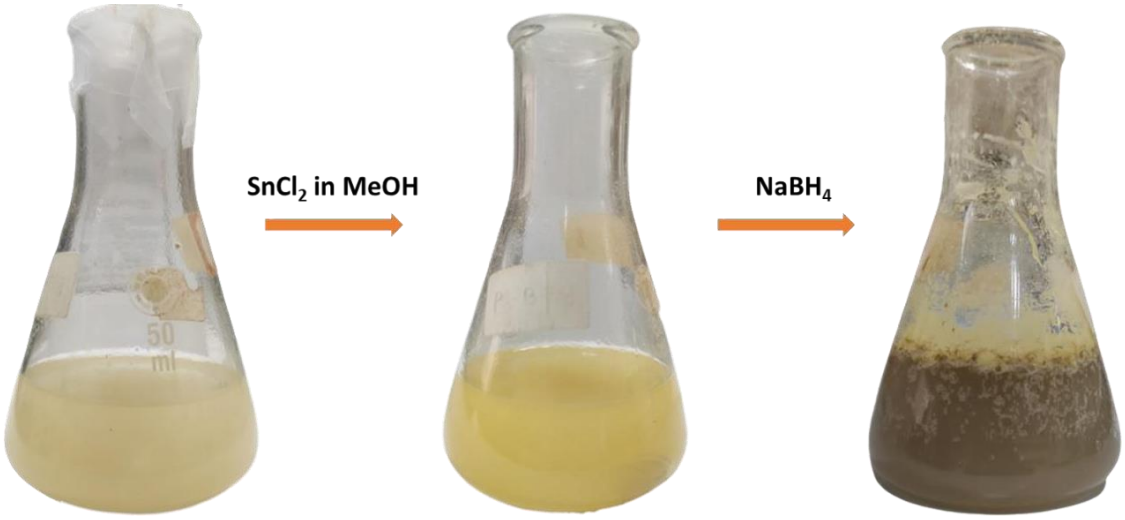

Scheme 3. SnO_2 loading in IISERP-COF6

3.2 Results

3.2.1 Characterization of 2,4,6-Tris-(4-formyl phenoxy)-1,3,5-triazine

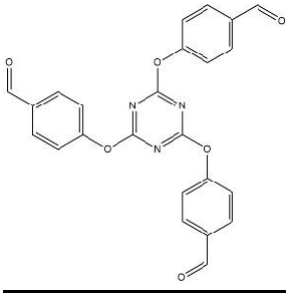

Fig 1. 2,4,6-Tris (4-formyl phenoxy)-1,3,5- triazine

^{1}H NMR (400 MHz, $CDCl_3$): δ = 9.99 (s, 3H), 7.92 (d, 6H), 7.32(d, 6H) (Please refer to Figure A1 A).
^{13}C NMR (101 MHz, $CDCl_3$): δ= 122.2(s), 131.3(s), 134.5(s), 155.7(s), 173.25(s), 190.59(s) (Please refer to Figure A1B).

3.2.2 Characterization of IISERP-COF6

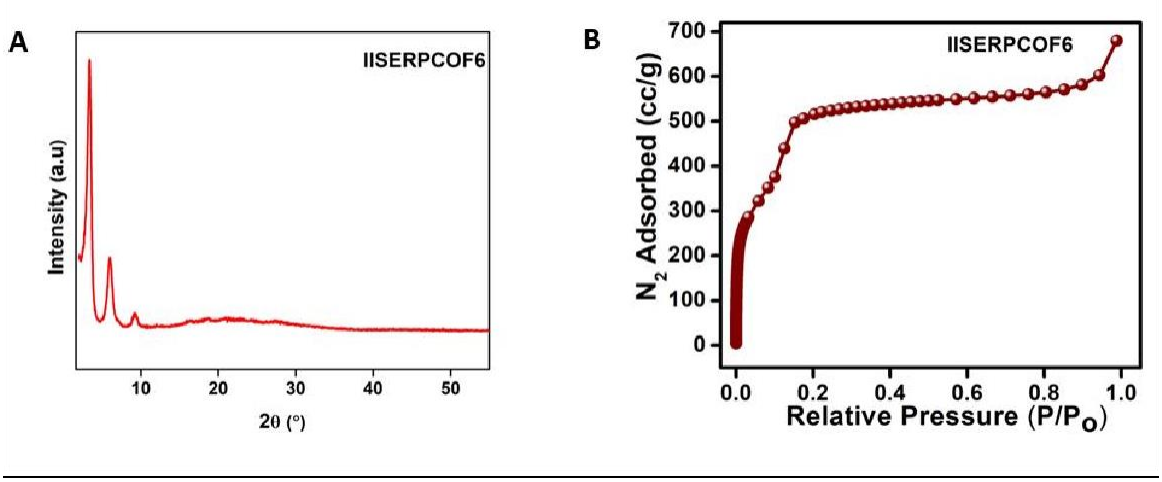

Fig 2 (A) PXRD of IISERP-COF6 (B) Nitrogen adsorption isotherm of IISERP-COF6 at 77K.

PXRD measurements were done to evaluate the crystallinity of the synthesized COF (Fig.2A). The characteristic low angle, high intensity peak confirms the formation of COF with pretty good crystallinity. N_2 adsorption at 77K was done to evaluate the permanent porosity of the synthesized COF. The BET surface area of the as-made COF's N_2 adsorption isotherm is 1440 m^2/g. The N_2 adsorption isotherm shows a type-II profile with a N_2 uptake of around 700 cc/g (Figure 2B). Excellent crystallinity shown in the PXRD is thought to be a reflection of the highly ordered structure that is responsible for this high uptake. FESEM studies shows that the COF has fluffy cotton like morphology (Fig. A3). EDAX analysis and Elemental mapping of COF were done (Fig. A4 (A,B)). The infrared (IR) spectroscopy stretching band at 1505 cm^{-1} corresponds to the vibration of C=N, Ar bonds and the stretching at 1627 cm^{-1} and 1366 cm^{-1} to the vibration of C=N and C=O bonds, respectively (Fig.3)

3.2.3 Characterization of SnO_2 loaded IISERP-COF6

The SnO_2 loaded IISERP-COF6 was subjected to PXRD to see what changes SnO_2 loading has brought to the COF framework and the crystallinity of the COF. To understand in what form Sn has been loaded in the pores of IISERP-COF6, SnO_2 loaded IISERP-COF6 was pyrolyzed under nitrogen and the PXRD and IR of the pyrolyzed sample was analyzed. The PXRD of this composite indicates that Sn has been loaded as SnO_2 nanoparticles in IISERP-COF6, as the peaks obtained in the pyrolyzed composites aligns well with the PXRD of SnO_2 nanoparticles.[19] The diffraction peak's intensities are broad and relatively weak compared to bulk SnO_2. This can be due to small crystallite size of SnO_2 nanoparticles. (Fig A2, A, B). As we can see from the PXRD data (Fig 3A), the crystallinity of IISERP-COF6 has dropped a bit compared to freshly prepared COF. This can be due to the harsh conditions which we used during loading of SnO_2 using double solvent method. The usage of strong reducing agent, $NaBH_4$ will probably the reason behind the drop in crystallinity of COF. FESEM images of SnO_2 loaded IISERP-COF6 depicts that there has been hardly any difference in the morphology of COF after SnO_2 loading. SnO_2 loaded IISERP-COF6 also showed a fluffy cotton like morphology (Fig.A5). Elemental mapping

confirms the homogenous distribution of SnO_2 nanoparticles throughout the COF frameworks (Fig. A6). Also, there was no peak corresponding to Sn or SnO_2 in the PXRD of SnO_2 loaded COF. So, to ascertain the presence of Sn, we have performed an EDAX analysis. From the EDAX data, we could infer that Sn has been successfully loaded into IISERP-COF6 with a weight percentage of 12 wt% (Fig. A7). Thus, the absence of Sn peaks in the Sn loaded IISERP-COF6 can be due to the reason that Sn might have been grown as small sized nanoparticles in the pores of COF, thus did not show any characteristic peak in the PXRD.[18]

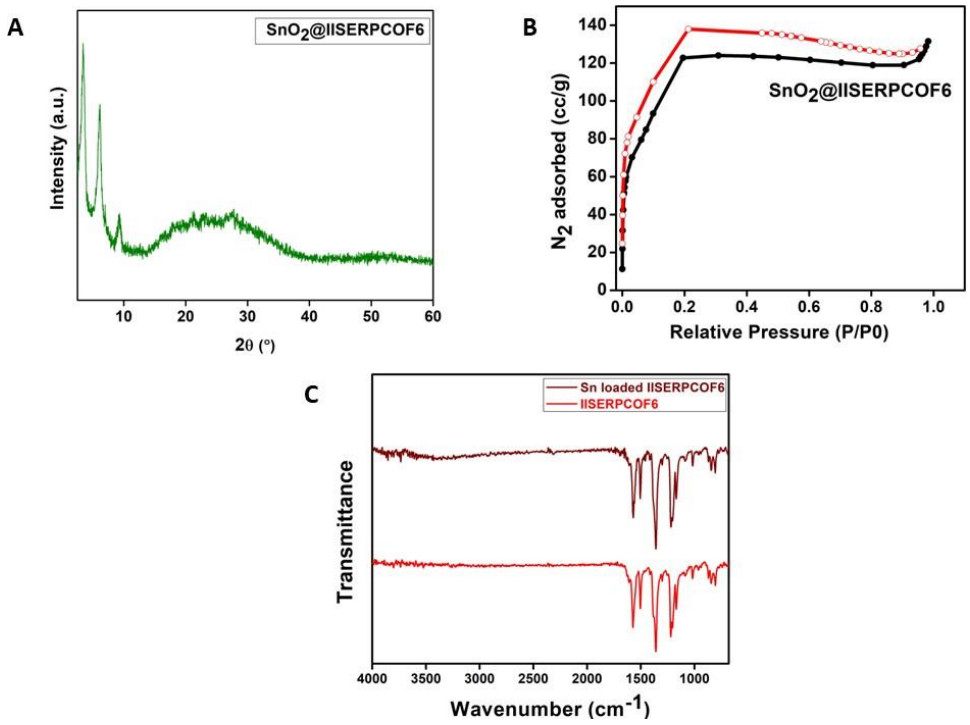

Fig 3(A) PXRD of SnO_2 loaded at IISERP-COF6 (B) Nitrogen adsorption isotherm of SnO_2 loaded at IISERP-COF6 at 77K (C) Comparison of IR spectrum of IISERP-COF6 and SnO_2 loaded IISERP-COF6.

There was a huge drop in the N_2 uptake of SnO_2 loaded IISERP-COF6. For the SnO_2 loaded IISERP-COF6, the N_2 uptake was just 140 cc/g. Also, the BET surface area and Langmuir surface area has reduced to 316 m^2/g (Fig.A8). This suggests that SnO_2 might have been loaded in the pores of IISERP-COF6. (Fig 3B). IR data of both IISERP-COF6 and SnO_2 loaded IISERP-COF6 has been measured to confirm whether COF has been able to maintain its structural integrity after using harsh conditions in double solvent method. IR data of both COF and SnO_2 loaded one are exactly similar indicating that the structure of the COF is intact and is stable towards the reduction procedure used in the Double Solvent method. The stretching at 1505 cm^{-1} corresponds to the vibration of C=N, Ar bonds and the stretching at 1627 $cm^{-1}$and 1366 cm^{-1} due to the vibration of C=N and C=O bonds were intact in the SnO_2 loaded IISERP-COF6(Fig.3C).

Appendix of Chapter 3

NMR of ligand

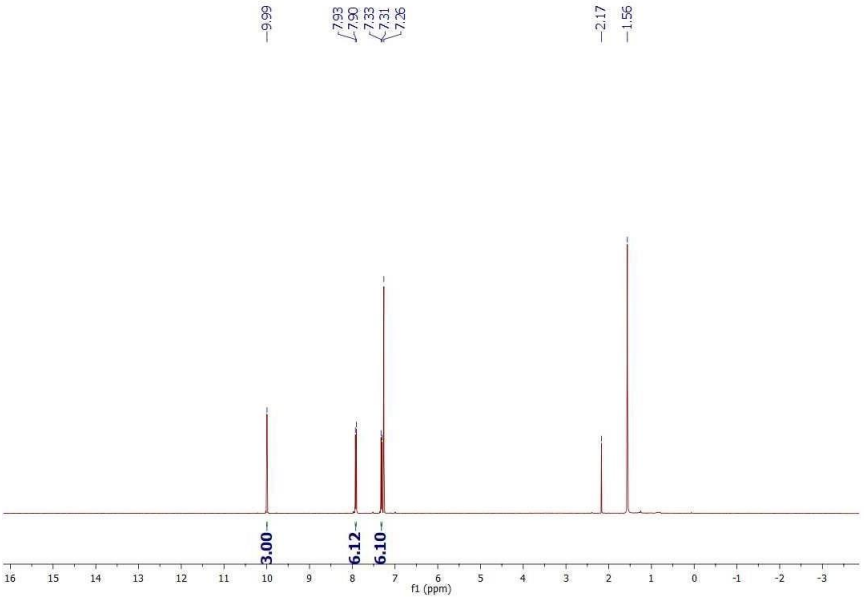

Figure A1. (A) ^{1}H NMR of 2,4,6-tris (4-formyl phenoxy),1,3,5, triazine showing characteristic peaks.

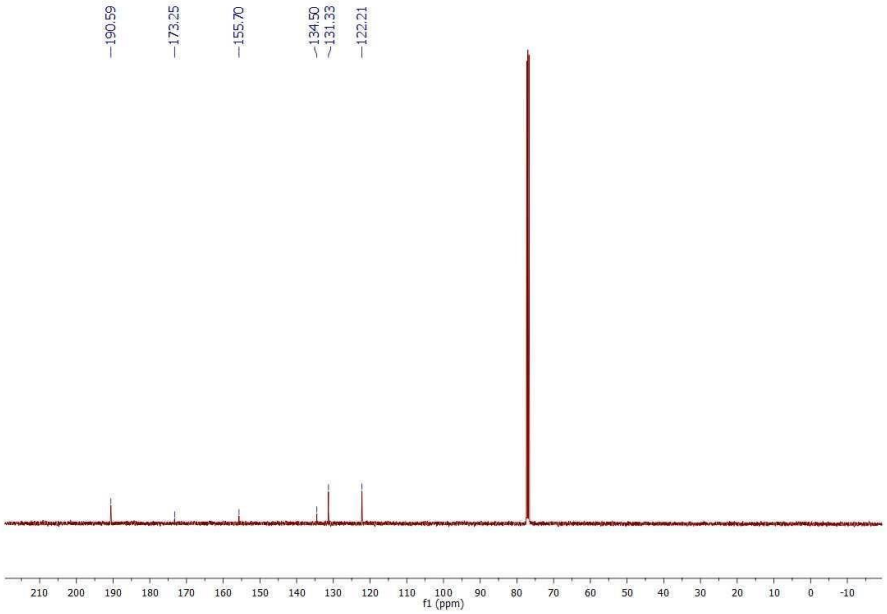

Figure A1 (B) ^{13}C NMR of 2,4,6-tris (4-formyl phenoxy)-1,3,5 triazine showing characteristic peaks.

Characterization of IISERP-COF6

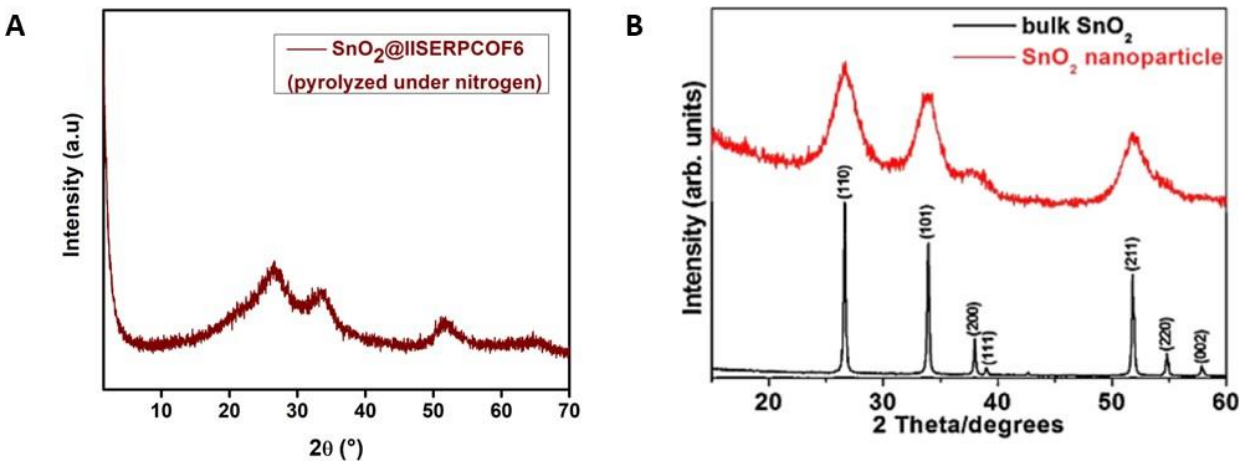

Fig A2 (A) PXRD of SnO_2 loaded in IISERP-COF6 pyrolyzed under nitrogen (B) PXRD of bulk SnO_2 and SnO_2 nanoparticles

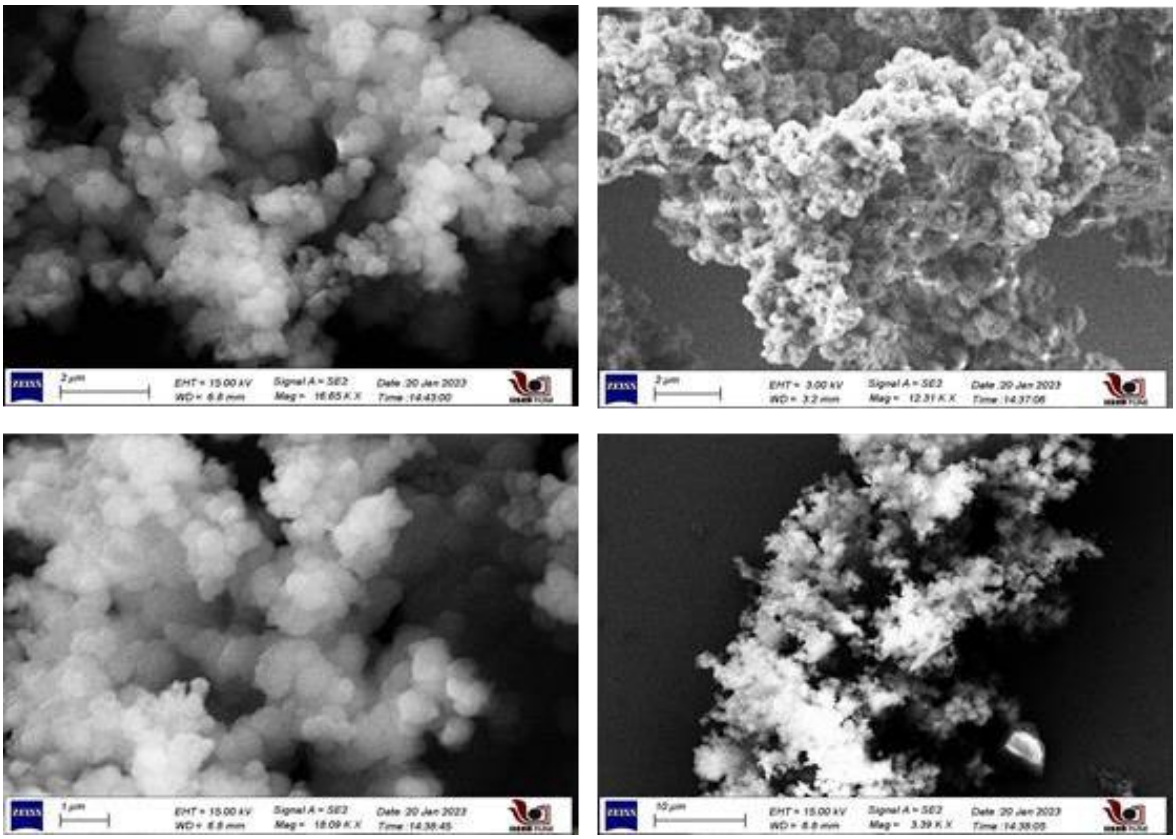

Fig. A3. FESEM images showing fluffy cotton like morphology of IISERP-COF6

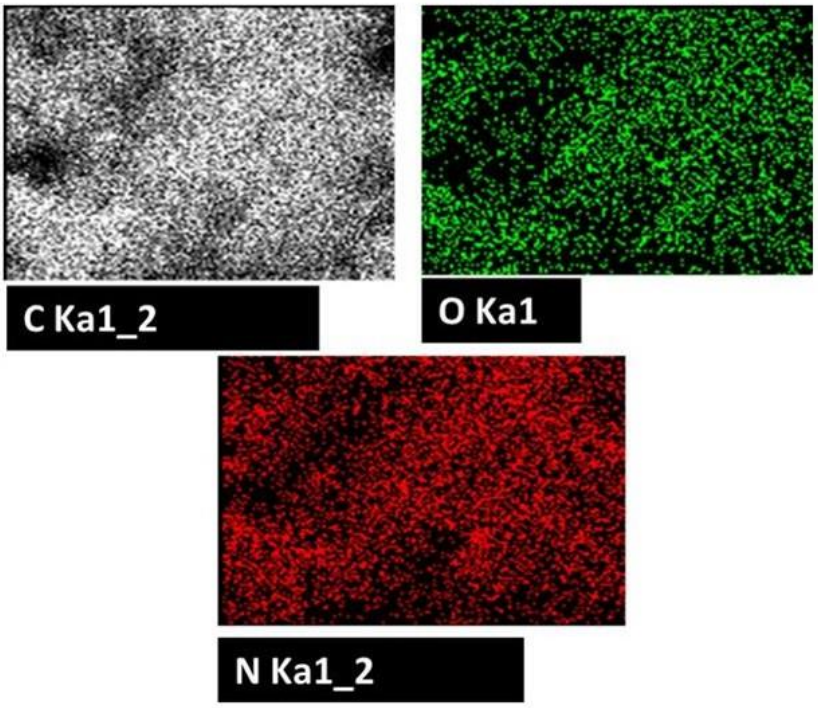

B

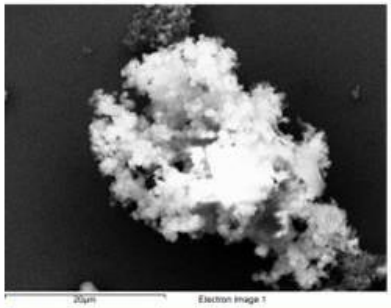

Element	Weight %	Atomic %
C K	69.94	74.30
N K	15.27	13.91
O K	14.79	11.79
Totals	100.00	

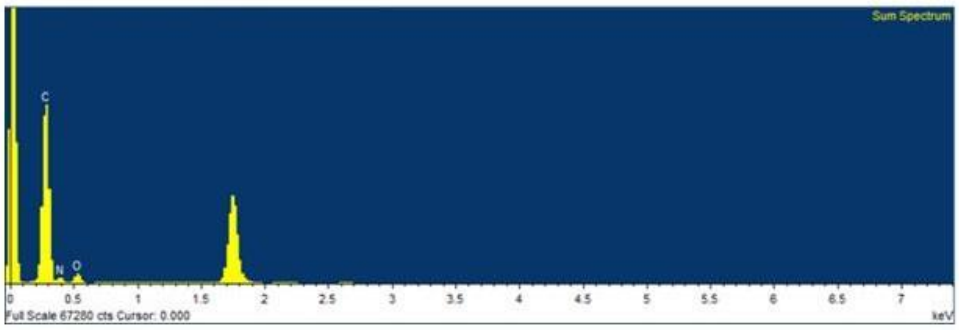

Fig. A4 (A) Elemental mapping image of IISERP-COF6 (B) EDAX of IISERP-COF6

Characterization of SnO_2@IISERP-COF6

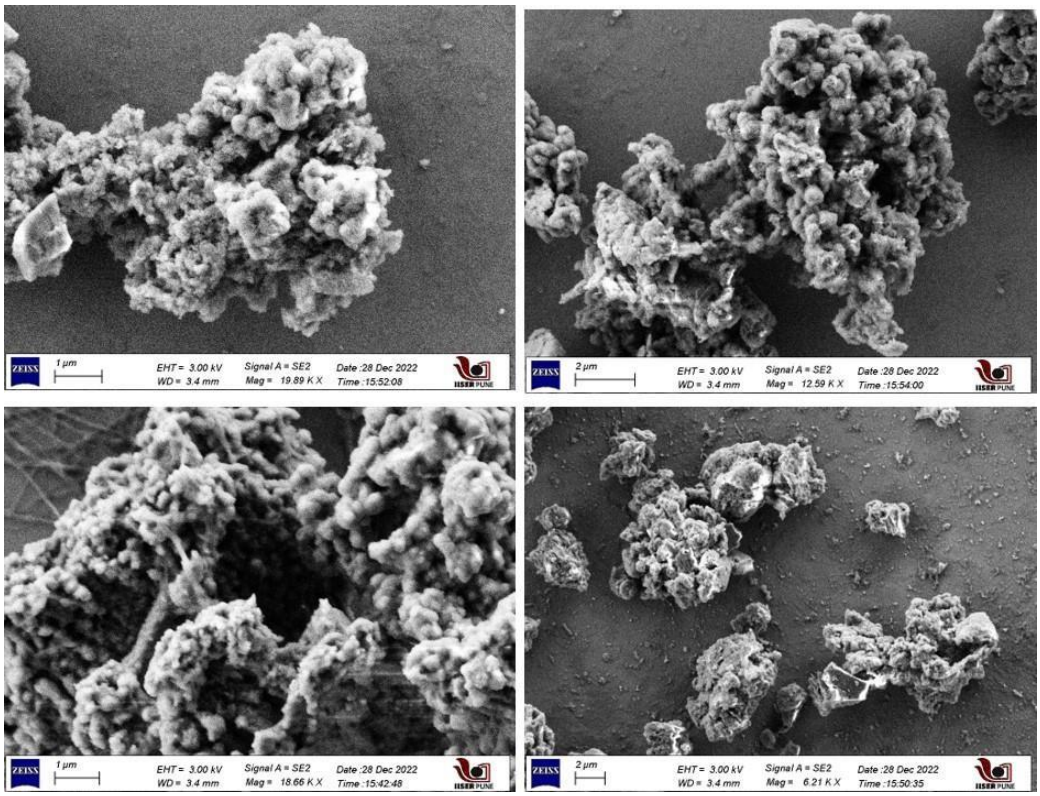

Fig A5. FESEM images of SnO_2 loaded at IISERP-COF6

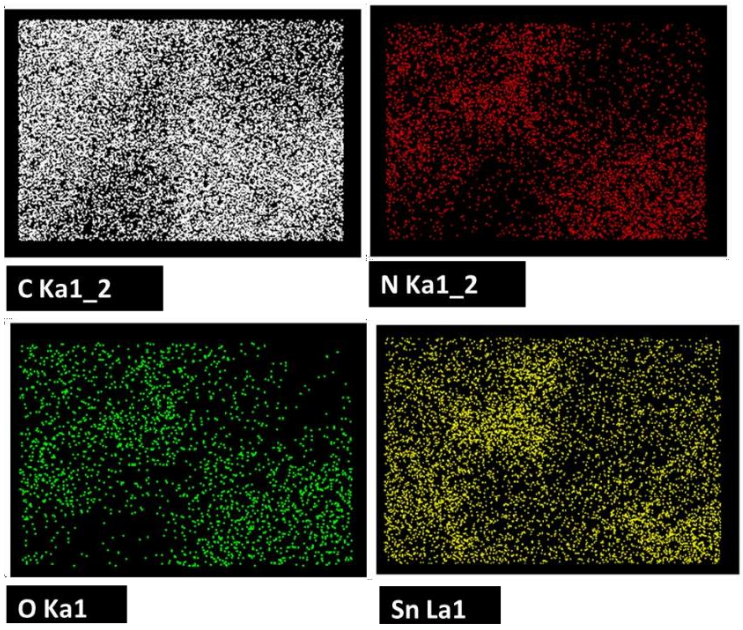

Fig.A6. Elemental mapping of SnO_2@IISERP-COF6

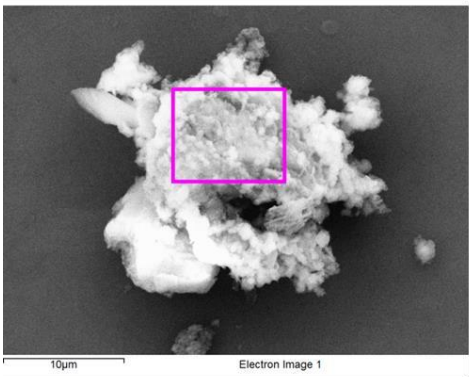

Element	Weight%	Atomic%
C K	47.03	58.94
N K	14.29	15.36
O K	25.54	24.03
Sn L	13.14	1.67
Totals	100	

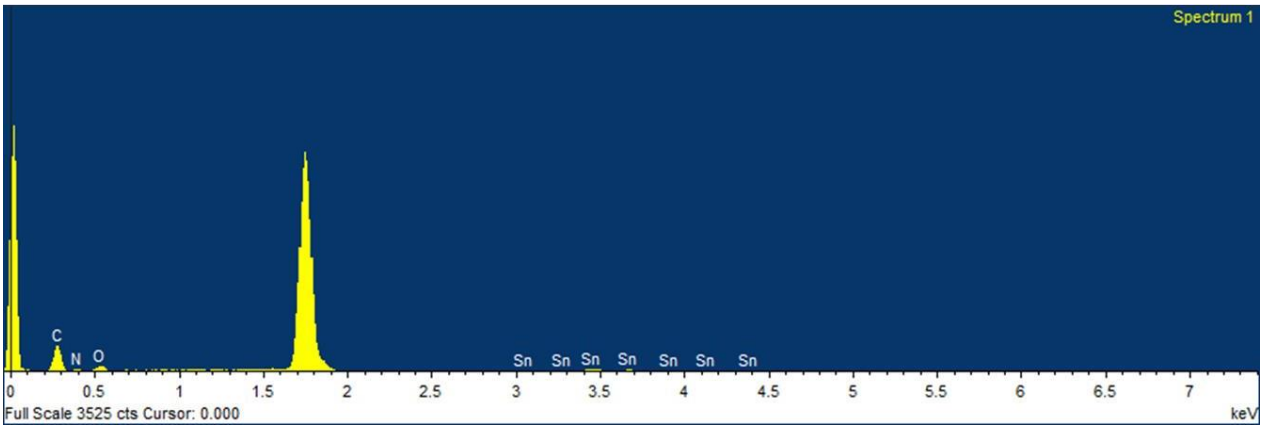

Fig.A7. EDAX analysis of SnO_2 loaded in IISERP-COF6

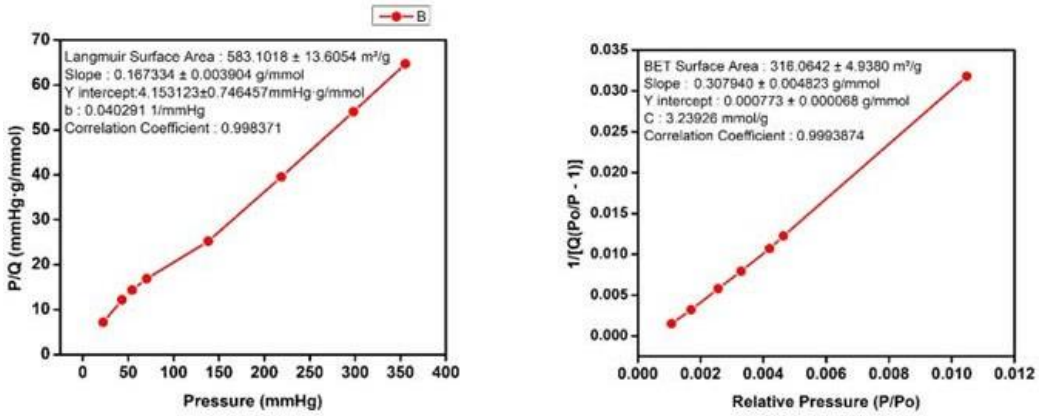

Fig.A8. Langmuir surface area and BET surface area of SnO_2 loaded in IISERP-COF6

Chapter 4: Electrochemistry

4.1 Cyclic voltammetry and Galvanostatic charge-discharge Cycling

Considering the advantage of porous framework with redox active groups and multiple organic functional groups (-OH, -C=N and aromatic carbons) which can interact with Li^+ ions and its advantage to buffer the volume change associated with SnO_2 during alloying/dealloying process and dispersing SnO_2 as nanoparticles, the potential of this material as an anode in LIB was investigated.

4.1.1 Fabrication of coin cell

To prepare the slurry, 75% SnO_2 loaded IISERP-COF6 (32.5 mg) (active material), 25% conducting carbon (12.5 mg) and 5% PVDF (5 mg) binder were grinded thoroughly in a clean mortar pestle. 0.6 ml N-methyl pyrrolidone (NMP) was added to make the slurry. It was then grinded thoroughly to form a highly viscous slurry. It was then coated on a copper foil (5*5 cm). Fig 1 shows the coin cell preparation. It was dried and hot cell pressed. After hot cell pressing, the electrode was cut according to 2032 type coin cell. The coin cell was fabricated inside the glove box using the above-mentioned electrode as the anode material, Li as cathode and $LiPF_6$ dissolved in 1:1 ethylene carbonate and dimethyl carbonate as the electrolyte. 2% (v/v) of flouro ethylene carbonate (FEC) was added to the electrolyte (Fig 2). The role of the FEC is to prevent the formation of SEI layer after the first discharge cycle.

Fig.1. Diagram showing coin cell preparation for electrochemical measurements

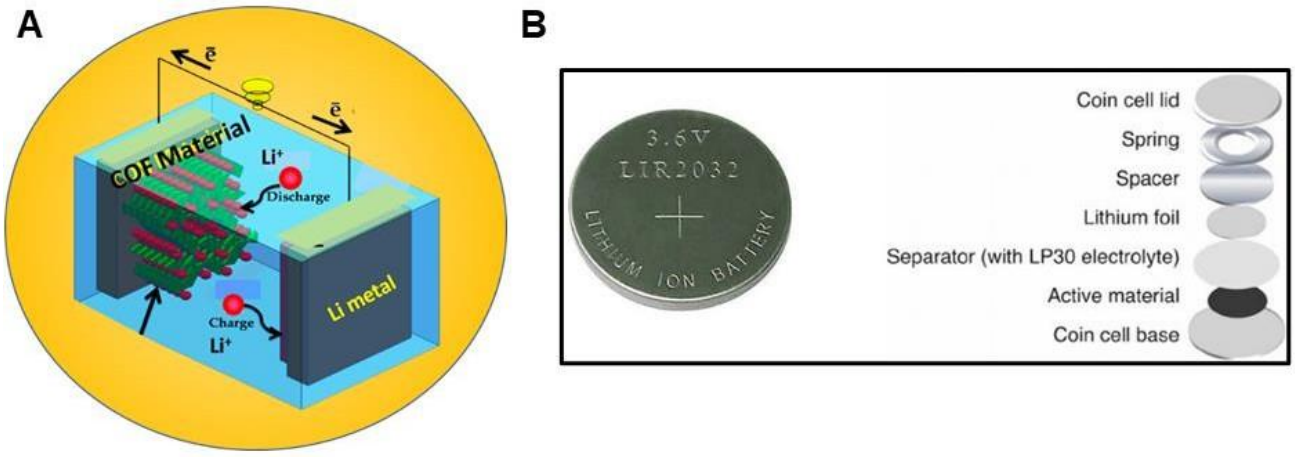

Fig 2 (A) Diagram showing Li ion intercalation during charge/discharge and (B) Coin cell assembly.

The Cyclic Voltammogram (CV) of coin cell was recorded at 0.1mV/s scan rate (Fig 3A). It was scanned in a potential window of 0.01-3V. The sharp peak at low potential (0.22V) indicates Li ion intercalation into the SnO_2 loaded IISERP-COF6. The broad peak at 0.56V corresponds to the alloying/ dealloying reaction of Li with Sn [Eq. (3)]. The peak at 1.25V corresponds to conversion reaction of SnO_2 [Eq. (4)]. Increase in current density with increase in scan rate indicates a capacitive behavior.[20]

$Sn + xLi^+ + xe^- \longleftrightarrow LixSn\ (0 < X < 4.4)$ [Eq. (3)]

$SnO_2 + 4Li^+ + 4e^- \longleftrightarrow Sn + 2\ Li_2O$ [Eq. (4)]

The fresh coin cell was also subjected to CV at different scan rates (Fig 3B).To learn more about the Li insertion de-insertion characteristics, the fabricated coin cell was connected to a galvanostatic charge discharge cycler and the specific capacity of coin cell was measured at 100mA/g current density. The specific capacity of the coin cell increased gradually over cycles and attained a specific capacity of 1100 mAh/g at 100 mA/g current density (Fig 3C). A coulombic efficiency of 100% was maintained throughout the 300 cycles (Fig 3D). The conversion reaction [Eq.(4)] was thought to be irreversible, but it can be made partially reversible for nanosized SnO_2. The reversibility of various reaction stages has a significant impact on the specific capacity of SnO_2 anodes. The theoretical maximum capacity of the entire reaction, which includes both conversion and alloying, is 1494 mAh/g, but if only the alloying/dealloying process is reversible, the maximum capacity drops to 783 mAh/g. An increased specific capacity (Fig 3D) for our material may be attributed to the partial reversibility of the conversion reaction.[21] An increase in specific capacity with prolonged cycling may be due to two reasons. It can be either because of the potential-driven steady activation of the favorable electrochemical sites for Li accommodation or more electrolyte is able to reach the pores of the active material.[22] An increase in specific capacity for Sn based systems have been reported previously in other works.[23,24]

Based on the previous reports, one plausible explanation for increase in specific capacity upon cycling can be proposed. Upon charge discharge, the Sn nanoparticles formed during conversion reaction become even smaller because of an effect called electrochemical force[25] and these particles will be

held more firmly by COF. It has been reported that when the reagent particle size decreases, the activation energy for solid state decomposition reaction also decreases.[26] Therefore the conversion reaction [(Eq.4)] which was earlier thought to be irreversible can become partially reversible as the sizes of the Sn has been reduced upon cycling. And the obtained capacity (around 110 mAh/g) which is quite higher than the theoretical capacity of only alloying/ dealloying reaction (783 mAh/g) further validates this theory.[27]

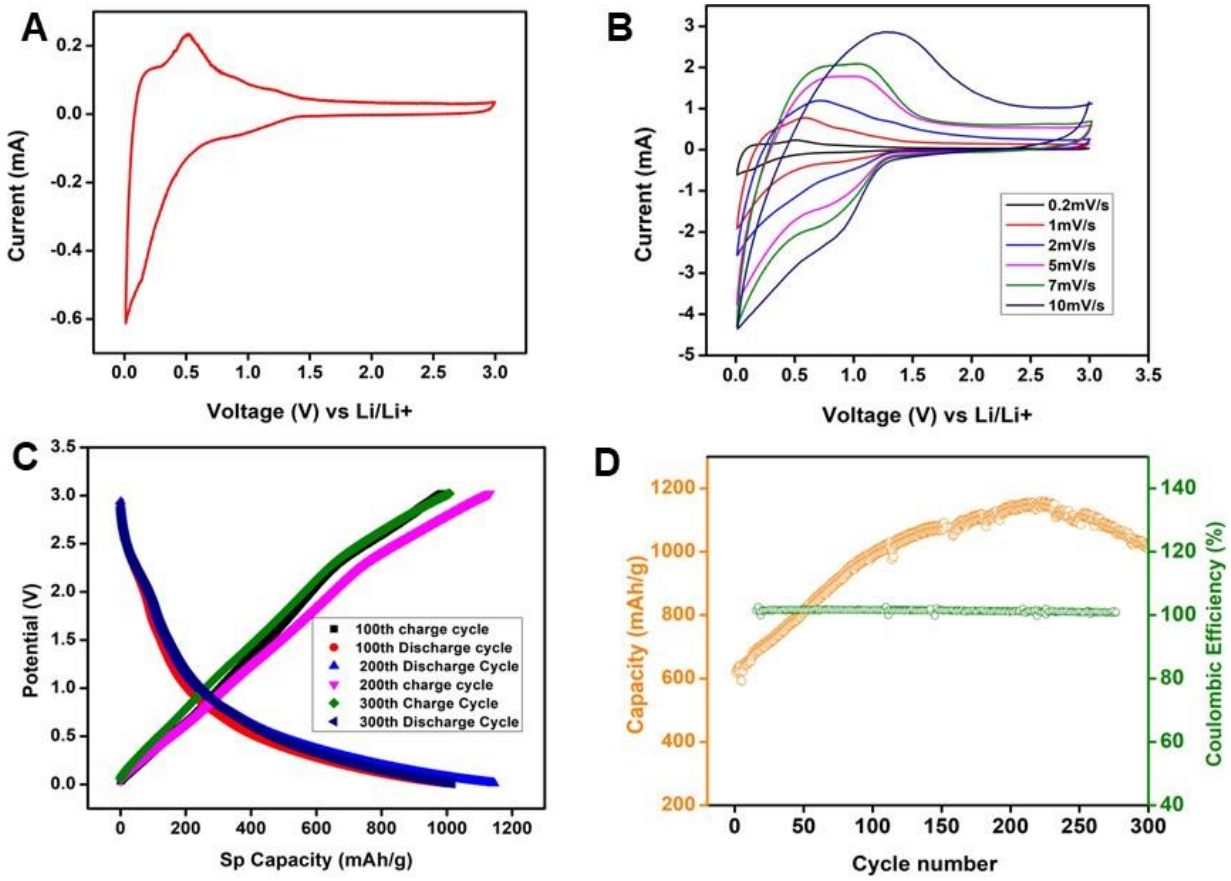

Fig.3 (A) CV of fresh coin cell measured at 0.1mV/s (B) CV of fresh coin cell measured at different scan rates. (C) Potential vs Specific capacity of SnO_2@IISERP-COF6 cell (D) Specific capacity and Coulombic efficiency of coin cell over 350 cycles

Conclusion

This work showcases the design of a high-capacity anode material for LIB by incorporating SnO_2 nanoparticles into a covalent organic framework, namely IISERP-COF6. The porous structure of COF makes it serve in the synthesis of capping-agent free nanoparticles or nanoclusters.[28] The intrinsically spongy nature of the COF will mitigate the volume changes associated with the alloying of Sn with Li during charge discharge. Here we have synthesized IISERP-COF6 with high crystallinity so that the COF will be able to sustain some crystallinity even after the treatment with strong reducing agent. SnO_2 nanoparticles were loaded inside the pores of COF support by using double solvent method. There has been a decrease in the N_2 uptake and BET surface area of the COF after loading SnO_2 indicating that SnO_2 has been loaded in the pores of IISERP-COF6. The morphology and structure of the COF remained intact before and after SnO_2 loading as confirmed by FESEM and IR analysis.

To study the properties of the material as an anode in LIB, a coin cell was fabricated using the SnO_2 loaded IISERP-COF6 as the anode material. The coin cell showed an OCV of 2.9V. The cell was connected to a charge discharge unit and the specific capacity of the coin cell was recorded. The specific capacity of the SnO_2@IISERP-COF6 loaded coin cell increased gradually upon cycling and attained a specific capacity of 1100 mAh/g. The increased specific capacity and the gradual increase upon cycling can be due to the conversion reaction becoming reversible with cycles, this reaction which was earlier thought to be irreversible. This reversibility contributes to the overall specific capacity of the material. Thus, the COF support not only mitigated the volume changes associated with Sn alloying/dealloying with Li, but also could firmly hold the small sized nanoparticles aiding the reversibility of the conversion reaction. Therefore, incorporating tin dioxide nanoparticle into a porous support is an effective strategy to develop high-capacity LIB anodes.

Reference

1. Geng, K.; He, T.; Liu, R.; Dalapati, S.; Tan, K. T.; Li, Z.; Tao, S.; Gong, Y.; Jiang, Q.; Jiang, D. Covalent Organic Frameworks: Design, Synthesis, and Functions. *Chem. Rev.* **2020***, 120* (16), 8814–8933.
2. Chen, X.; Geng, K.; Liu, R.; Tan, K. T.; Gong, Y.; Li, Z.; Tao, S.; Jiang, Q.; Jiang, D. Covalent Organic Frameworks: Chemical Approaches to Designer Structures and Built-In Functions. *Angewandte Chemie International Edition* **2020***, 59* (13), 5050–5091.
3. Bhambri, H.; Khullar, S.; Sakshi; K. Mandal, S. Nitrogen-Rich Covalent Organic Frameworks: A Promising Class of Sensory Materials. *Materials Advances* **2022***, 3* (1), 19–124.
4. Kandambeth, S.; Dey, K.; Banerjee, R. Covalent Organic Frameworks: Chemistry beyond the Structure*. J. Am. Chem. Soc.* **2019,** *141* (5), 1807–1822.
5. Deng, L.; Ding, Z.; Ye, X.; Jiang, D. Covalent Organic Frameworks: Chemistry of Pore Interface and Wall Surface Perturbation and Impact on Functions. *Acc. Mater. Res.* **2022***, 3* (8), 879–893.
6. Zhao, X.; Pachfule, P.; Thomas, A. Covalent Organic Frameworks (COFs) for Electrochemical Applications. *Chem. Soc. Rev.* **2021***, 50 (12),* 6871–6913.
7. Guo, F.; Zhang, W.; Yang, S.; Wang, L.; Yu, G. 2D Covalent Organic Frameworks Based on Heteroacene Units. *Small*, 2207876.
8. Kong, X.; Zhou, S.; Strømme, M.; Xu, C. Redox Active Covalent Organic Framework-Based Conductive Nanofibers for Flexible Energy Storage Device. *Carbon* **2021***, 171,* 248–256.
9. Tong, Y.; Wang, X.; Zhang, Y.; Huang, W. Recent Advances of Covalent Organic Frameworks in Lithium-Ion Batteries. *Inorg. Chem. Front.* **2021,** *8* (3), 558–571.
10. Chae, S.; Choi, S.-H.; Kim, N.; Sung, J.; Cho, J. Integration of Graphite and Silicon Anodes for the Commercialization of High-Energy Lithium-Ion Batteries*. Angewandte Chemie International Edition* **2020***, 59* (1), 110–135.
11. Kebede, M. A. Tin Oxide–Based Anodes for Both Lithium-Ion and Sodium-Ion Batteries. *Current Opinion in Electrochemistry* **2020***, 21*, 182–187.
12. Liu, L.; Xie, F.; Lyu, J.; Zhao, T.; Li, T.; Choi, B. G. Tin-Based Anode Materials with Well-Designed Architectures for next-Generation Lithium-Ion Batteries*. Journal of Power Sources* **2016,** *321,* 11–35.
13. Belliard, F.; Connor, P. A.; Irvine, J. T. S. Novel Tin Oxide-Based Anodes for Li-Ion Batteries. *Solid State Ionics* **2000**, *135* (1), 163–167.
14. Xin, F.; Whittingham, M. S. Challenges and Development of Tin-Based Anode with High Volumetric Capacity for Li-Ion Batteries. *Electrochem. Energ. Rev.* **2020**, *3* (4), 643–655.
15. Tahmassebi, D. C.; Sasaki, T. Synthesis of a New Trialdehyde Template for Molecular Imprinting*. J. Org. Chem*. **1994**, *59* (3), 679–681.
16. Kushwaha, R.; Kaleeswaran, D.; Haldar, S.; Chakraborty, D.; Mullangi, D.; Borah, A.; Vinod, C. P.; Murugavel, R.; Vaidhyanathan, R. Nanoporous Covalent Organic Framework Embedded

with Fe/Fe3O4 Nanoparticles as Air-Stable Low-Density Nanomagnets. *ACS Appl. Nano Mater*. **2020**, *3* (9), 9088–9096.

17. Mullangi, D.; Chakraborty, D.; Pradeep, A.; Koshti, V.; Vinod, C. P.; Panja, S.; Nair, S.; Vaidhyanathan, R. Highly Stable COF-Supported Co/$Co(OH)_2$ Nanoparticles Heterogeneous Catalyst for Reduction of Nitrile/Nitro Compounds under Mild Conditions. *Small* **2018**, *14* (37), 1801233.
18. Mullangi, D.; Nandi, S.; Shalini, S.; Sreedhala, S.; Vinod, C. P.; Vaidhyanathan, R. Pd Loaded Amphiphilic COF as Catalyst for Multi-Fold Heck Reactions, C-C Couplings and CO Oxidation. *Sci Rep* **2015**, *5*, 10876.
19. Kim, S. P.; Choi, M. Y.; Choi, H. C. Photocatalytic Activity of SnO_2 Nanoparticles in Methylene Blue Degradation. *Materials Research Bulletin* **2016**, *74*, 85–89.
20. Yi, L.; Liu, L.; Guo, G.; Chen, X.; Zhang, Y.; Yu, S.; Wang, X. Expanded Graphite@SnO2@ Polyaniline Composite with Enhanced Performance as Anode Materials for Lithium Ion Batteries. *Electrochimica Acta* **2017**, *240,* 63–71.
21. Zoller, F.; Böhm, D.; Bein, T.; Fattakhova-Rohlfing, D. Tin Oxide Based Nanomaterials and Their Application as Anodes in Lithium-Ion Batteries and Beyond. *ChemSusChem* **2019**, *12* (18), 4140–4159.
22. Mahajan, M.; Roy, K.; Parmar, S.; Singla, G.; Pandey, O. P.; Singh, K.; Vaidhyanathan, R.; Ogale, S. Room Temperature Processed In-Situ Carbon-Coated Vanadium Carbide (VC@C) as a High Capacity Robust Li/Na Battery Anode Material. *Carbon* **2020**, *161*, 108–116.
23. Zhang, N.; Zhao, Q.; Han, X.; Yang, J.; Chen, J. Pitaya-like Sn@C Nanocomposites as High-Rate and Long-Life Anode for Lithium-Ion Batteries. *Nanoscale* **2014**, *6* (5), 2827–2832.
24. Xu, Y.; Guo, J.; Wang, C. Sponge-like Porous Carbon/Tin Composite Anode Materials for Lithium Ion Batteries. *J. Mater. Chem.* **2012**, *22* (19), 9562–9567.
25. Yu, Y.; Shi, Y.; Chen, C.-H.; Wang, C. Facile Electrochemical Synthesis of Single-Crystalline Copper Nanospheres, Pyramids, and Truncated Pyramidal Nanoparticles from Lithia/Cuprous Oxide Composite Thin Films. *J. Phys. Chem. C* **2008**, *112* (11), 4176–4179.
26. Taberna, P. L.; Mitra, S.; Poizot, P.; Simon, P.; Tarascon, J.-M. High Rate Capabilities Fe3O4-Based Cu Nano-Architectured Electrodes for Lithium-Ion Battery Applications. *Nature Mater* **2006**, *5* (7), 567–573.
27. Lian, P.; Zhu, X.; Liang, S.; Li, Z.; Yang, W.; Wang, H. High Reversible Capacity of SnO2/Graphene Nanocomposite as an Anode Material for Lithium-Ion Batteries. *Electrochimica Acta* **2011**, *56* (12), 4532–4539.
28. Ramanathan, V.; MULLANGI, D.; Nandi, S. Covalent Organic Frameworks as Porous Supports for Non-Noble Metal Based Water Splitting Electrocatalysts. US10301727B2, May 28, 2019.
29. Luo, Z.; Liu, L.; Ning, J.; Lei, K.; Lu, Y.; Li, F.; Chen, J. A Microporous Covalent–Organic Framework with Abundant Accessible Carbonyl Groups for Lithium-Ion Batteries. *Angewandte Chemie International Edition* **2018**, *57* (30), 9443–9446.

30. Hu, Y.; Wayment, L. J.; Haslam, C.; Yang, X.; Lee, S.; Jin, Y.; Zhang, W. Covalent Organic Framework Based Lithium-Ion Battery: Fundamental, Design and Characterization. *EnergyChem* ***2021****, 3* (1), 100048
31. Zhu, D.; Xu, G.; Barnes, M.; Li, Y.; Tseng, C.-P.; Zhang, Z.; Zhang, J.-J.; Zhu, Y.; Khalil, S.; Rahman, M. M.; Verduzco, R.; Ajayan, P. M. Covalent Organic Frameworks for Batteries. *Advanced Functional Materials* **2021**, *31* (32), 2100505
32. Weeks, J. A.; Sun, H.-H.; Srinivasan, H. S.; Burrow, J. N.; Guerrera, J. V.; Meyerson, M. L.; Dolocan, A.; Heller, A.; Mullins, C. B. Facile Synthesis of a Tin Oxide-Carbon Composite Lithium-Ion Battery Anode with High Capacity Retention. *ACS Appl. Energy Mater.* **2019**, *2* (10), 7244–7255
33. Haldar, S.; Roy, K.; Nandi, S.; Chakraborty, D.; Puthusseri, D.; Gawli, Y.; Ogale, S.; Vaidhyanathan, R. High and Reversible Lithium Ion Storage in Self-Exfoliated Triazole-Triformyl Phloroglucinol-Based Covalent Organic Nanosheets. *Advanced Energy Materials* **2018**, *8* (8), 1702170
34. Haldar, S.; Roy, K.; Kushwaha, R.; Ogale, S.; Vaidhyanathan, R. Chemical Exfoliation as a Controlled Route to Enhance the Anodic Performance of COF in LIB. *Advanced Energy Materials* **2019**, *9* (48), 1902428